Laboratory Report No. BNL 9213 (unpublished).
[4]G. Cocconi, V. T. Cocconi, A. D. Krisch, J. Orear, R. Rubinstein, D. B. Scarl, B. T. Ulrich, W. F. Baker, E. W. Jenkins, and A. L. Read, Phys. Rev. 138, B165 (1965).
[5]R. Serber, Rev. Mod. Phys. 36, 649 (1964).
[6]A. D. Krisch, Phys. Rev. 135, B1456 (1964).
[7]D. E. Damouth, L. W. Jones, and M. L. Perl, Phys. Rev. Letters 11, 287 (1963).
[8]M. L. Perl, Y. Y. Lee, and E. Marquit, Phys. Rev. 138, B707 (1965).
[9]L. M. Simmons, Phys. Rev. Letters 12, 229 (1964).
[10]G. Fast and R. Hagedorn, Nuovo Cimento 27, 208 (1963).
[11]G. Fast, R. Hagedorn, and L. W. Jones, Nuovo Cimento 27, 856 (1963).

BACKWARD ELASTIC SCATTERING OF HIGH-ENERGY PIONS BY PROTONS*

W. R. Frisken, A. L. Read,† and H. Ruderman

Brookhaven National Laboratory, Upton, New York

and

A. D. Krisch

The University of Michigan, Ann Arbor, Michigan,
and Laboratory of Nuclear Studies, Cornell University, Ithaca, New York

and

J. Orear, R. Rubinstein, D. B. Scarl, and D. H. White

Laboratory of Nuclear Studies, Cornell University, Ithaca, New York
(Received 24 June 1965)

A backward peak in the positive pion-proton elastic cross section has been reported[1] for 4-GeV/c incident pions as well as a hint that this peak might persist at higher energies.[2] We have studied backward elastic scattering of pions at 4 and 8 GeV/c, measuring cross sections for positive and negative pions at center-of-mass angles from 170° to 180° in the center of mass. We find a sharp peak in the backward direction for positive pions and a lower, flatter peak for negative pions at both 4 and 8 GeV/c.

The experimental arrangement was similar to that used in an experiment to measure forward elastic cross sections at high momentum transfers, which is reported in the preceding Letter.[3] Figure 1 shows the arrangement used for backward scattering. The backward-scattered pion and the forward-going proton were each momentum analyzed and detected in scintillation-counter telescopes. The solid angle in the center of mass, subtended by each telescope, ranged from 0.5 to 1.5 msr; the momentum resolution ranged from ±6 to ±12%. From two to five scattering angles were measured at one time, using a large fraction of the 120-in. by 24-in. gap of the pion magnet and the 30-in. by 6-in. gap of the proton magnet.

A threshold gas Cherenkov counter together

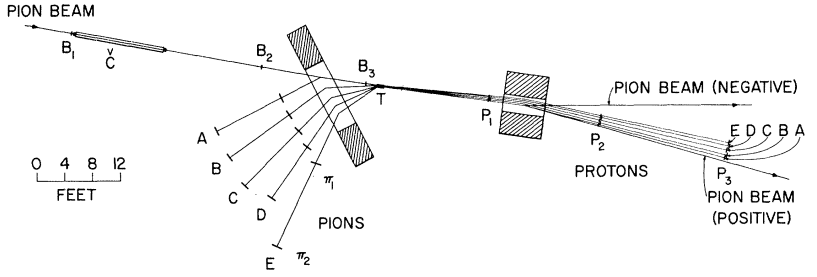

FIG. 1. The experimental arrangement. B_1, $\check{C}$, B_2, and B_3 are the incident beam defining counters and T is the hydrogen target. π_1 and π_2 are the counters of the five pion telescopes, and P_1, P_2, and P_3 are the counters of the five proton telescopes. The incident pion beam passes through the large-aperture magnet before striking the target.

with three scintillation counters was used to identify pions in the incident beam. Coincidences between the beam counters, a proton telescope, and the corresponding pion telescope were used to gate signals from the last counters in the pion and proton telescopes. These signals were put into a time to height converter whose output spectrum was recorded by a pulse-height analyzer. The peak in the spectrum corresponding to the time of arrival of real elastic events allowed those events to be separated from the accidental events which were not correlated in time and appeared as a uniform background. This technique supplemented standard coincidence counting and was useful at 8 GeV/c, where the accidental background subtraction amounted to up to 75% of the counting rate. At 4 GeV/c the accidental rate was negligible.

The data were corrected for the 8% of muons and electrons in the incident beam, for the 11% absorption of the scattered pions and recoil protons in the scintillation counters, hydrogen target, and air, for the loss due to decay in flight of 14% of the 0.4-GeV/c backward-scattered pions, and for a 3% empty-target counting rate. The large number of protons in the positive beams could not simulate pion events since it is kinematically impossible for an incident proton to scatter beyond 90° in the laboratory system. The contribution of inelastically scattered pions to the measured cross sections was estimated by counting crossed-channel events in which a pion telescope was put into coincidence with an uncorrelated proton telescope, and also by running with liquid nitrogen in place of liquid hydrogen in the target. In all cases the inelastic contamination was estimated to be less than 5%.

The errors given with the data are partly statistical and include the 10% uncertainty in the above correction factors. A 10% uncertainty in the solid angles for backward scattering is also included since the focusing of the pions in the fringe field of the large-aperture bending magnet made the accepted solid angles very sensitive to variations in magnet current.

The measured values of $d\sigma/d\Omega$, the differential elastic cross section, versus $\cos\theta_{\text{c.m.}}$, the center-of-mass scattering angle, are given in Table I and plotted in Figs. 2 and 3 together with some previous data at smaller angles for comparison. At 4 GeV/c the extrapolated positive pion cross section at 180° is about 2×10^{-3} the height of the forward diffraction peak. The extrapolated backward positive cross section is about a factor of three lower at 8 GeV/c than at 4 GeV/c. The negative pion cross sections near 180° are about 7 times smaller than the positive peaks and seem to be flat within the errors at both 4 and 8 GeV/c.

In order to compare the width of the forward and backward peaks in π^+-p scattering we have fit the backward cross sections with the function

$$d\sigma/dt = (d\sigma/dt)_{t=t_{\max}} \exp[\alpha(t_{\max}-t)],$$

where t is the invariant four-momentum transfer squared, and $t_{\max}$ is the value of t at 180°. This results in an α of 17 ± 3 $(\text{GeV}/c)^{-2}$ for the

Table I. The measured elastic-scattering cross sections.

Incident particle	p_0 (GeV/c)	$\theta_{\text{c.m.}}$	$\cos\theta_{\text{c.m.}}$	$(d\sigma/d\Omega)_{\text{c.m.}}$ (μb/sr)	$-t$ (GeV/c)^2	$d\sigma/dt$ [μb/(GeV/c)^2]
π^-	4	177.5°	−0.9991	6.8 ± 1.4	6.695	12.7 ± 2.6
		175.0°	−0.9962	9.2 ± 1.6	6.686	17.3 ± 3.0
		170.0°	−0.9848	8.1 ± 1.5	6.648	15.2 ± 2.8
π^+	4	175.0°	−0.9962	52.1 ± 8.4	6.686	98 ± 16
		170.0°	−0.9848	35.2 ± 5.7	6.648	66 ± 11
π^-	8	180.0°	−1.0000	2.68 ± 0.65	14.160	2.38 ± 0.58
		177.5°	−0.9991	4.30 ± 0.99	14.154	3.81 ± 0.88
		175.0°	−0.9962	1.88 ± 0.49	14.133	1.67 ± 0.44
		172.5°	−0.9914	2.89 ± 0.70	14.100	2.56 ± 0.62
		170.0°	−0.9848	2.34 ± 0.56	14.053	2.08 ± 0.50
π^+	8	177.5°	−0.9991	14.6 ± 4.4	14.154	13.0 ± 3.9
		175.0°	−0.9962	10.4 ± 1.9	14.133	9.2 ± 1.7
		172.5°	−0.9914	6.6 ± 1.5	14.100	5.9 ± 1.3
		170.0°	−0.9848	2.30 ± 0.71	14.053	2.04 ± 0.64

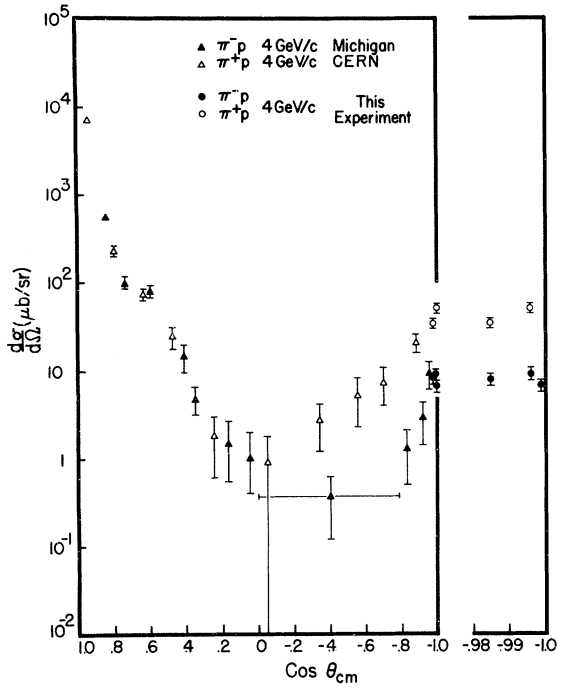

FIG. 2. A plot of the elastic pion-proton cross sections at 4 GeV/c. Near $\cos\theta = -1$, the data are replotted on an expanded scale to show the shape of the backward peaks. The Michigan data are from C. Coffin, N. Dikmen, L. Ettlinger, D. Meyer, A. Saulys, K. Terwilliger, and D. Williams, to be published; the CERN data are from reference 1.

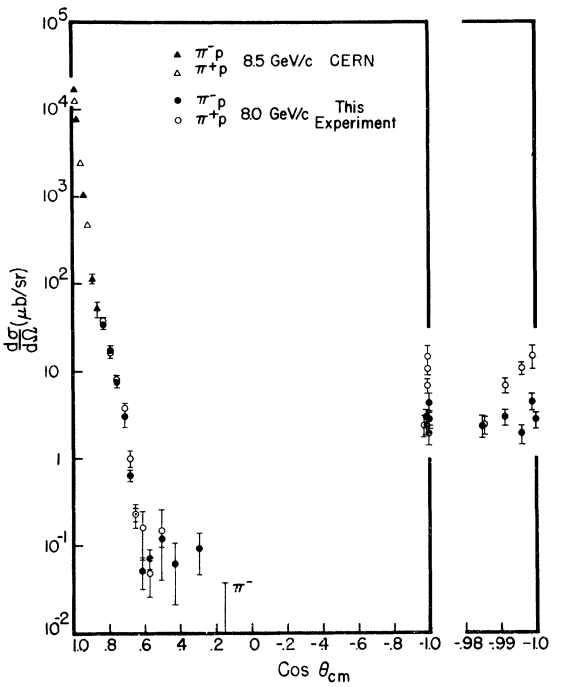

FIG. 3. A plot of the elastic pion-proton cross sections at 8 GeV/c. Near $\cos\theta = -1$, the data are replotted on an expanded scale to show the shape of the backward peaks. The CERN data are from reference 6. The 8-GeV/c data in the forward direction are from reference 3.

8-GeV/c cross sections and an α of 11 ± 6 (GeV/c)$^{-2}$ for the two points at 4 GeV/c. The function

$$d\sigma/dt = (d\sigma/dt)_{t=0} e^{At}$$

is known to fit the forward peak well with $A = 8 \pm 1$ (GeV/c)$^{-2}$ for incident momenta from 2 to 18 GeV/c.[1,4-6] The errors are sufficiently small to conclude that the backward peak in 8-GeV/c π^+-p scattering is narrower than the forward diffraction peak. This may not be inconsistent with a diffraction theory,[7] but the charge dependence of the backward peak seems to imply that the backward scattering may be due to a process more complicated than simple diffraction.

A model involving the exchange of a neutron for π^+-p backward scattering and of a doubly charged isobar for π^--p scattering could account for the π^- cross section falling below the π^+ cross section. Unfortunately, calculations of single-particle exchange do not agree with either the height or the width of the backward peaks.[8] Allowing multiple-particle exchange or making absorptive corrections to the single-particle exchange[9] help to bring the predictions closer to the experimental data, but further calculations and data are needed to test the exchange hypothesis.

We would like to express our appreciation to the administration and staff of the Brookhaven AGS for their assistance and cooperation which made possible the performance of this experiment.

---

*Research supported in part by the U. S. Atomic Energy Commission and the National Science Foundation. This research was performed using the alternate gradient synchrotron at Brookhaven National Laboratory.

†Presently on leave of absence at the Lawrence Radiation Laboratory, University of California, Berkeley, California.

[1]Aachen-Berlin-Birmingham-Bonn-Hamburg-London-Munchen Collaboration, Phys. Letters 10, 248 (1964).

[2]M. Deutschman, D. Kropp, S. Nagel, H. Weber, W. Woischnig, C. Grote, J. Klugow, S. Nowak, S. Brandt, V. T. Cocconi, O. Csyzewski, J. Danysz,

P. Dalpiaz, G. Kellner, and D. R. O. Morrison, CERN Publication No. 64-31 (unpublished).

[3]J. Orear, R. Rubinstein, D. B. Scarl, D. H. White, A. D. Krisch, W. R. Frisken, A. L. Read, and H. Ruderman, preceding Letter [Phys. Rev. Letters 15, 309 (1965)].

[4]K. J. Foley, S. J. Lindenbaum, W. A. Love, S. Ozaki, J. J. Russell, and L. C. L. Yuan, Phys. Rev. Letters 11, 425 (1963).

[5]D. E. Damouth, L. W. Jones, and M. L. Perl, Phys. Rev. Letters 11, 287 (1963).

[6]D. Harting, E. Elsner, D. O. Caldwell, A. C. Helmholz, W. C. Middelkoop, B. Zacharov, P. Dalpiaz, S. Focardi, G. Giacomelli, L. Monari, J. A. Beaney, R. A. Donald, P. Mason, and L. W. Jones, Nuovo Cimento 13, 60 (1965).

[7]M. L. Pearl, L. W. Jones, and C. C. Ting, Phys. Rev. 132, 1252 (1963).

[8]V. Cook, B. Cork, W. R. Holley, and M. L. Perl, Phys. Rev. 130, 762 (1963).

[9]Richard M. Heinz and Marc H. Ross, Phys. Rev. Letters 14, 1091 (1965).

RARE DECAY MODES OF THE η MESON AS A PROBE OF ELECTROMAGNETIC AND STRONG INTERACTIONS*

Donald A. Geffen and Bing-lin Young

School of Physics, University of Minnesota, Minneapolis, Minnesota

(Received 28 June 1965)

The rare decay modes of the η meson,

$$\eta \to \mu^+ + \mu^- + \gamma, \tag{1}$$

$$\eta \to e^+ + e^- + \gamma, \tag{2}$$

$$\eta \to \mu^+ + \mu^- \tag{3}$$

can provide a variety of valuable information about electromagnetic and strong interactions. In particular, three things can be learned.

(1) A comparison of decay modes (1) and (2), for the same values of the lepton-pair center-of-mass energy, tests for a difference between the muon-photon and electron-photon interaction for timelike virtual photon momenta.

(2) The measurement of the distribution of events in Reactions (1) and (2), as a function of lepton-pair center-of-mass energy, yields the "electromagnetic form factor" of the meson. The result can then be compared with the predictions of SU(3).

(3) The branching ratio for decay mode (3), $R(\eta \to \mu^+ + \mu^-/\eta \to 2\gamma)$, depends strongly upon the behavior of the $\eta \to 2\gamma$ vertex for large virtual photon momenta.

Since it is now fairly certain that the η meson is pseudoscalar,[1] the phenomenological descriptions of decay modes (1), (2), and (3) are completely analogous to that for the corresponding decays of the π^0 meson.[2-4] Assuming conventional quantum electrodynamics for both the electron and muon, we can write the invariant matrix element for decay processes (1) and (2),

$$T = [eF_\eta(Q^2/m_\eta^2)/m_\pi Q^2] \times \epsilon_{\mu\nu\lambda\tau}\epsilon^\mu k^\nu q^\lambda \bar{u}(p_-)\gamma^\tau v(p_+). \tag{4}$$

$\bar{u}$ and v are the appropriate spinors for the negative and positive muons or electrons with momenta p_- and p_+, q is the η momentum, k the photon momentum, and ϵ the polarization. $Q^2 = (p_+ + p_-)^2$. The form factor F_η is the amplitude for a real η meson to decay into a real photon and a virtual photon of mass $(Q^2)^{1/2}$. The factor of m_π, the π^0 mass, has been introduced to make F_η dimensionless, and is so chosen in order to facilitate the comparison of η decay with π^0 decay. Expression (4) for T leads to the well-known Dalitz-pair decay rate,[5]

$$\frac{d\Gamma_{\eta\to\gamma+l^+l^-}}{dX} = \Gamma_{\eta\to 2\gamma}\left(\frac{2\alpha}{3\pi}\right)\left|\frac{F_\eta(X)}{F_\eta(0)}\right|^2\left(\frac{X-4m_l^2/m_\eta^2}{X}\right)^{1/2}\left(\frac{X+2m_l^2/m_\eta^2}{X^2}\right)(1-X)^3, \tag{5}$$

with $4m_l^2/m_\eta^2 \le X = Q^2/m_\eta^2 \le 1$. The decay rates for Reactions (1) and (2) are obtained from Eq. (5) by setting m_l equal to the muon and electron masses, m_μ and m_e, respectively. It is seen immediately from Eq. (5) that the ratio of muon to electron Dalitz pairs, for fixed X, is predicted unambiguously by quantum electrodynam-